ARTICLES

Gas Diffusion in Polycrystalline Silicalite Membranes Investigated by ^{1}H Pulse Field-Gradient NMR

Hiromitsu Takaba,*,† Atsushi Yamamoto,† Kikuko Hayamizu,‡ and Shin-ichi Nakao†

Department of Chemical System Engineering, The University of Tokyo, 7-3-1 Hongo Bunkyo-ku, Tokyo 113-8685, Japan, and National Institute of Advanced Industrial Science and Technology, AIST Tsukuba Center 5, Tsukuba 305-8565, Japan

Received: November 3, 2004; In Final Form: April 24, 2005

^{1}H pulse field-gradient (PFG) spin−echo NMR was performed to measure the diffusivity of methane in a polycrystalline MFI-type silicalite membrane. Measured diffusivities decreased with an increase in the diffusion distance and converged to the constant value. This result suggests the presence of a transport barrier in the membrane. The long-time diffusivity in the membrane was 3.7×10^{-9} m^2/s, which was a factor of 3 smaller than reported values in a single crystal. The distance between the transport barriers was estimated to be much larger than 6 μm from the relationship of diffusivity with displacement. It should be noted that the estimated distances were larger than the smallest dimension of the crystals appearing in the membrane surface. Gas permeation and pervaporation tests were carried out on the same sample for which NMR measurements were taken. The estimated methane flux using measured long-time diffusivity by the permeation theory overestimated the experimental value, although it is closer to the experimental value than the value estimated using the short-time diffusivity. These results mean that the methane diffusivity in a silicalite membrane is much smaller than that in a single crystal.

Introduction

Mass transport in zeolite membranes is of fundamental importance in a variety of applications as a separation technique based on their molecular sieving and preferential adsorption properties. Zeolite membranes are usually prepared as thin layers of an assembly of small zeolite crystals, including numerous intercrystalline regions. The intercrystalline regions will influence the properties of the membrane, e.g., the separation factor and permeance; however, the relationship between the structure of the intercrystalline region and the membrane's performance is still not fully understood. This is probably because of the difficulty in characterizing the intercrystalline regions by direct experimental methods. The size of the intercrystalline region is in the range of a few nanometers, which is beyond the resolution of a scanning electron microscope.

Gravimetric, volumetric, and barometric techniques and pulse field-gradient (PFG) NMR have been used to measure diffusivities of various gases in zeolites.[1] Because PFG-NMR measurements respond to diffusivities on a microscopic scale, in contrast to the other techniques, the measured diffusivity can be related to the microscopic structures. Intracrystalline structure that affects diffusivity of small adsorbates was recently evaluated by the use of PFG-NMR. Vasenkov et al. reported that the diffusivity of *n*-butane in an MFI-type zeolite single crystal decreased with an increase in the measuring diffusion time, even if the diffusion distance was shorter than the crystal size.[2] We observed that the diffusivity of methane decreased as the result of the existence of small cracks in a single crystal by PFG-NMR.[3] These results suggest that intracrystalline structures, e.g., defects, imperfect crystallinity, and interfaces, significantly affect the gas diffusivity. The diffusivity of ethane and propane in a Ca exchanged A-type zeolite membrane was investigated as a function of diffusion distance.[4] The diffusivities of both species for large diffusion displacement were a factor of 2 or 3 smaller than that in a crystalline NaCaA, where the diffusion displacement was much smaller than the sample size, which means that the transport barrier at the outer surface of the sample did not influence the diffusion. However, the common feature of the relationship between membrane performance and transport properties of zeolite membranes, as well as the difference from transport properties in a single crystal, is not clear.

A difference of transport properties in zeolite membranes from those in crystals has been implied from the inconsistency between theoretical studies and experiments. Molecular simulations have been carried out to estimate the permeability in zeolite membranes to compare with the experimental data by using the perfect crystal model to model the zeolite membrane.[5−8] For example, we applied permeation theory combined with molecular simulation to estimate the permeabilities of inorganic gases (CH_4, Ar, He, Ne, N_2, and O_2) in high-silica MFI-type zeolite membranes (silicalite) at 301 K.[5,6] The results showed that the calculated permeabilities were about 1 order of magnitude larger than the experimental values, although the dependence on the

* Corresponding author. E-mail: takaba@chemsys.t.u-tokyo.ac.jp.
† The University of Tokyo.
‡ National Institute of Advanced Industrial Science and Technology.

10.1021/jp044966z CCC: $30.25
Published on Web 07/01/2005

molecular weight of the permeating gases agreed with the experiment. Bowen et al. reported that adjusting the membrane thickness to obtain agreement between the predicted value of permeability and the experimental value led to a membrane thickness greater than that observed from a scanning electron microscopy (SEM) picture.[8] As shown by these studies, the permeability calculated by molecular modeling is likely to be an overestimate. These molecular simulations were based on interatomic interactions; parameters were adjusted to reproduce the diffusivity of species in a perfect zeolite crystal obtained from short-range diffusivity in crystallite by PFG-NMR. Therefore, to understand the reason for this discrepancy and for accurate estimation of the performance of zeolite membranes, the difference between the diffusivity in a single crystal and that in zeolite membranes should be clarified.

In this study, we carried out ^{1}H PFG-NMR to measure methane gas diffusivity in polycrystalline zeolite membranes (MFI-type silicalite), in order to clarify the difference in the diffusivity from that in a single crystal. The gas permeation and pervaporation measurements were also carried out for the zeolite membrane used in the PFG-NMR measurements to correlate the diffusivity with membrane performance. To our knowledge, this is the first report to measure gas diffusivity in zeolite membranes in which membrane performance is characterized.

Experimental Details

a. Synthesis of Silicalite Membrane. For NMR measurements, a large crystal (at least 20 μm) with low contamination from a support layer is required. Several synthesis techniques for MFI-type silicalite membranes have been reported, e.g., an in situ crystallization technique[9] and a secondary growth technique.[10,11] We chose the in situ crystallization technique for preparation of the silicalite membrane because using this method it is easier to obtain a thick membrane. The silicalite membranes were formed on a stainless steel disk, from which the synthesized membrane can be peeled.

MFI-type silicalite crystals were synthesized by an in situ crystallization using tetrapropylammonium bromide (TPABr), as a structure directing agent (SDA), and a colloidal silica (Cataloid SI-30 from Shokubai Kasei Co., Japan), as a silica source.[9] TPABr and colloidal silica were mixed and stirred for 3 h at room temperature to obtain a gel having a molar composition of 1 SiO_2:0.1 TPABr:0.05 Na_2O:80 H_2O. The hydrogel was poured into a 300-mL Teflon-lined autoclave. A porous stainless steel disk of 5-cm diameter with an average pore diameter of 10 μm was used as a support. The support was placed at the bottom of the autoclave. The autoclave was heated in an air-heated oven for 48 h. After the hydrothermal synthesis, the silicalite membrane was washed with pure water and calcined in air at 773 K for 20 h to remove the SDA.

The membrane morphology was examined using a scanning electron microscope (ESEM-2700, Nikon Instech Co., Ltd). The Brunauer−Emmett−Teller (BET) surface area and micropore volume were measured using an ASAP2010 (Shimadzu Inc.).

b. Permeation Measurements. The performance of the membrane was measured before the NMR measurements. The pervaporation measurement was made for an aqueous ethanol solution at 303 K, where the feed concentration of ethanol was 10−40 wt %. The liquid feed was circulated between the membrane cell and a large feed vessel, which kept the feed stream at a constant composition. In the membrane cell, the active surface area of the disk membrane was 3.8×10^{-4} m^2. The vacuum side was maintained at less than 0.3 Torr during the pervaporation using a vacuum pump. Permeate samples were collected by the use of a liquid nitrogen cold trap. The total flux was determined from the amount of permeate sample collected over a given time period. The permeate concentrations were analyzed by gas chromatography (Hewlett-Packard 6850A). The separation on concentration factor was determined using the following equation:

$$S_{ij} = \frac{y_{ip}/y_{jp}}{y_{if}/y_{jf}} \tag{1}$$

where y_{if} is the concentration of species i at the feed side and y_{ip} is the concentration of species i at the permeate side.

Measurements of single gas permeance through the membranes were also carried out for methane, *n*-butane, and isobutane. Permeance was measured as the pressure change of the evacuated permeate side compartment at 303 K. The feed pressure was kept between 1.0×10^{-5} and 1.1×10^{-5} Pa.

c. ^{1}H PFG-NMR Measurements. The disk-shaped silicalite membrane was shocked to peel the silicalite layer from the support. Because of the weak adhesion between stainless steel and silicalite, the membrane was separated by a relatively soft hit on the support without any damage to the surface of the support. The peeled silicalite layer was broken into small pieces about 2−3 mm in size, in order to fit into an NMR tube. The pieces were introduced into 5.0-mm-o.d. glass NMR tubes. The tubes were then degassed under vacuum at 673 K for at least 24 h. After cooling to room temperature, a controlled pressure methane gas (3×10^4 Pa) was introduced into the tube at 303 K. After achieving adsorption equilibrium, the tubes were carefully flame-sealed, avoiding any contamination from air. In this way, the adsorption site occupancy, θ, of methane in silicalite in the tube was approximately 0.1; the loading was 1.5−2.0 molecules per unit cell.

The diffusion measurements were carried out on a proton resonance PFG-NMR JEOL GSH-200 spectrometer with a 4.7 T wide-bore magnet controlled by a TecMag Apollo system. A JEOL current amplifier was used to generate the gradient pulses, g. In our measured system, the NMR spin−lattice relaxation time, T_1, was much larger than the spin−spin relaxation time, T_2, of methane; for example, T_1 and T_2 values at 243 K were 69 ms and 3.2 ms, respectively. Therefore, the stimulated echo pulse sequence (i.e., 90°−g−90°−τ−90°−g−acq) was used for the diffusion measurements. The echo attenuation, E, is related to the experimental variables by

$$E = \exp(-\gamma^2 g^2 \delta^2 D(\Delta - \delta/3)) \tag{2}$$

[12] where δ is the duration of the gradient pulse, Δ is the interval between the leading edges of the two gradient pulses, γ is the magnetogyric ratio, and D is the self-diffusivity of the molecules. The measurements were made by holding g at 9.2 T m^{-1} while altering δ between 0.01 and 0.25 ms, where the shape of the rectangle PFG was good enough to obtain reasonable data. The time Δ covered the range from 0.5 to 4 ms. The 90° pulse width was 9.1 μs. The time interval between the first two 90° pulses in the stimulated echo pulse sequence was 0.4 ms. The temperature range investigated was from 173 to 243 K, with the accuracy of temperature control in the measurements on the order of ±1.0 K.

Results and Discussion

a. Membrane. Figure 1 shows SEM microphotographs of the silicalite membrane. The surface view (a) shows that the

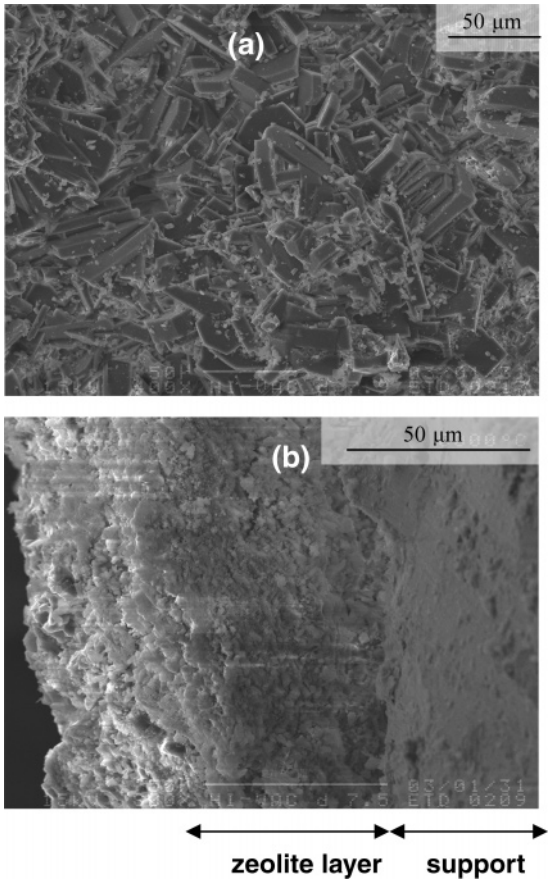

Figure 1. SEM images of the prepared MFI-type silicalite membrane; (a) is the surface view and (b) is the cross-sectional view.

zeolite layer consists of small zeolite crystals. Their sizes are approximately 5 μm × 5 μm × 30 μm. In photograph (b), larger crystals are observed close to the surface compared with those near the support, indicating an asymmetric structure. The estimated membrane thickness from photograph (b) is approximately 50 μm.

The measured BET surface area and micropore volume for the pieces of broken membrane that were peeled off the support were 329 m^2/g and 0.13 cm^3/g, respectively. It has been reported that the BET surface area and micropore volume of single silicalite crystals were 372−419 m^2/g and 0.17−0.19 cm^3/g, respectively, which depend on the synthesis conditions.[13] The BET surface area and micropore volume of the present sample were relatively smaller, compared with the reported values, by 10−20%. This means that the synthesized membrane has relatively low crystallinity compared with that of a single crystal.

b. Permeation. The result of the pervaporation for ethanol/water mixtures is presented in Figure 2. The flux increases with an increase in the ethanol concentration in the feed, and the flux and separation factor at a feed ethanol concentration of 10 wt % were 0.1 kg m^{-2} h^{-1} and 25, respectively. The measured single gas permeance values for methane, *n*-butane, and isobutane were 1.4 × 10^{-7}, 8.6 × 10^{-9}, and 4.4 × 10^{-9} mol m^{-2} s^{-1} Pa^{-1}, respectively. The present zeolite membrane had lesser or similar separation performance compared with that in the previous reports.[9,14]

c. PFG-NMR. The normalized attenuation curves for methane according to eq 2 at various Δ values are presented in Figure 3. The temperature was 173 K. If the diffusion is free in a homogeneous medium (Fickian diffusion), the plot is a straight line and the self-diffusion constant can be obtained from the gradient. As shown in Figure 3, the profiles for Δ = 0.5 and

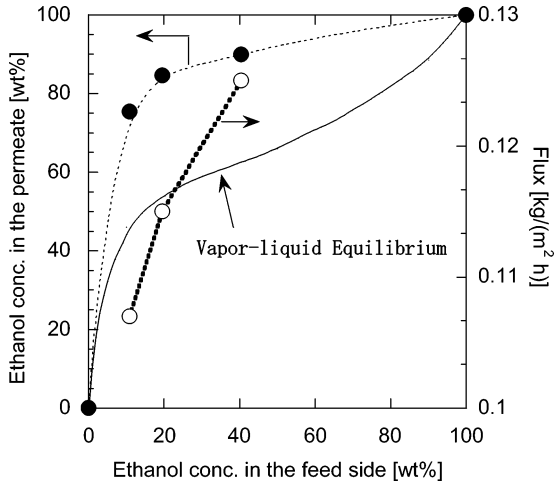

Figure 2. Pervaporation results for the silicalite membrane using aqueous ethanol solutions. (●) is the ethanol concentration in the permeate, and (○) is the flux. The solid line is the vapor−liquid line, shown to demonstrate the membrane selectivity.

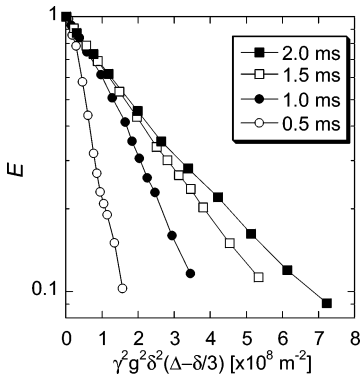

Figure 3. Normalized PFG-NMR spin−echo attenuation curves for methane at 173 K. The values in the inset list the values of Δ.

1.0 ms are not exactly straight, and they show a slightly convex shape. As the value of Δ increases (>1.5 ms), the profile becomes straight and changes to slightly concave, finally. The different behaviors of these profiles, depending on the value of Δ, imply that the zeolite membrane has inhomogeneous spaces for the diffusing methane molecules.

For further investigation of the observed diffusion behavior, additional measurements were performed at various temperatures at Δ = 0.5 ms. To draw an analogy to restricted diffusion, we tried to plot using an equation of the following form:

$$E = \exp(-(2\pi q)^2 D) \tag{3}$$

where $q = \gamma g \delta (2\pi)^{-1}$. The attenuation curve for diffusion in a heterogeneous structure is complex and known to sometimes exhibit diffraction behavior at well-defined values of *q*. The results are plotted in Figure 4. As shown in this figure, the curves were nonstraight at the investigated temperatures. This implies that the diffusion occurred in inhomogeneous spaces for this time scale of Δ.

The diffusivity can be estimated from the attenuation profile in Figure 3 using eq 2. The results are shown in Figure 5 as a function of the diffusion time at various temperatures. Strictly speaking, the diffusivities can be determined only when the attenuation curve is given by a single straight line. The attenuation curves for Δ = 0.5 and 1.0 ms are not straight; thus, we made the estimation of the diffusivities for the plots for which Δ's were larger than 1.5 ms, where the slopes were

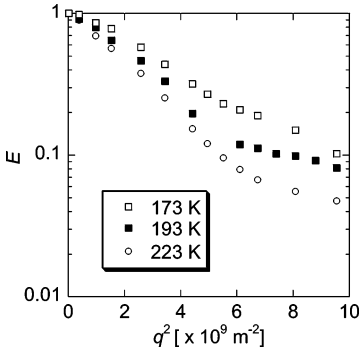

Figure 4. Normalized PFG-NMR spin−echo attenuation curves for methane at various temperatures. The value of Δ for the three measurements is 0.5 ms.

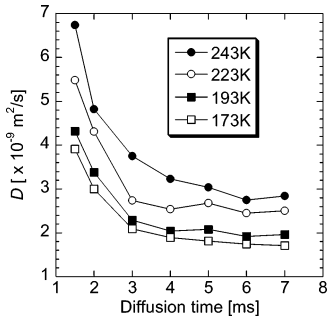

Figure 5. Relationship between the estimated diffusion coefficients of methane and the diffusion time at various temperatures.

reasonably assumed to be straight. The diffusivities at all temperatures in this figure show a strong decay and then become constant with an increase in the diffusion time. The observed drastic decreases in the diffusivities suggest the existence of a transport barrier in the membrane. The diffusivities at a short diffusion time (Δ = 1.5 ms) originate from diffusion in the intracrystalline region. For the diffusion time from 2 to 4 ms, the diffusivities decrease probably because the diffusing gases go through noncrystalline spaces in the zeolite. The diffusivities converge as the diffusion time increases because the contribution of diffusion in the noncrystalline spaces to the apparent diffusivity is averaged. The long-time diffusivity would be considered a practical diffusivity in the zeolite membranes.

The number of molecules that experienced the diffusion through the noncrystalline spaces become large as the diffusion time increases. An intercrystalline region or a defect space in the zeolite framework can be considered a noncrystalline space. It has been pointed out that desorption from the crystal to the intercrystal region decreased the diffusivity of hydrocarbons in NaX from the intracrystalline diffusivity by 2 orders of magnitude,[15] and Geier et al. showed that the interparticle boundary of NaX beds decreased the diffusivity of *n*-hexane.[16] Similar interface effects on diffusivity might work in the present system.

Table 1 shows a comparison of the measured diffusivity with the short-time diffusivity in the single crystal. The measured diffusivity in this table was converted to the self-diffusivity, D_s, using $D_s = D/(1 - \theta)$ to eliminate the dependence of diffusivity, D, on the site occupancy,[1] θ. The loading was calculated from the adsorption equilibrium in the NMR sample tube using the adsorption isotherm of methane in silicalite at each temperature. By comparing the reported short-time diffusivities obtained by PFG-NMR for single crystals, the long-time diffusivity in the membrane is reduced by a factor of 3. The reported diffusivities in single crystals from PFG-NMR and

TABLE 1: Comparison of Self-Diffusivity of Methane in a Silicalite Membrane with that in a Single Silicalite Crystal[a]

	method	temp [K]	D_s (long-time/short-time) [$\times 10^{-9}$ m^2/s]
this work	PFG-NMR	173	2.2/5.0
		193	2.4/5.4
		223	2.9/6.4
		243	3.1/7.6
		301	3.7[b]/8.8[b]
Jobic[17]	QENS	250	4.8
Caro et al.[18]	PFG-NMR	300	11−14
June et al.[19]	MD	300	16
Suzuki et al.[6]	MD	301	16
Talu et al.[20]	single-crystal membrane (diffusivity along *c*-axis)	323	4.1

[a] Long- and short-time D_s values were calculated from the attenuation plots at Δ = 7 ms and Δ = 1.5 ms, respectively. [b] Interpolation using observed activation energy.

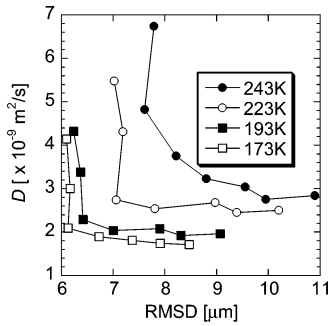

Figure 6. Relationship between the estimated diffusion coefficients of methane and the RMSD at various temperatures.

QENS agree reasonably with our estimated short-time diffusivities at Δ = 1.5 ms. This reasonable correspondence implies that the difference in diffusivities for the membrane compared with single crystals is due to the micrometer-order structural difference.

Using the long-time diffusivities at different temperatures, the activation energy for the diffusion is estimated to be 1.8 ± 0.1 kJ/mol. This value is smaller than the reported activation energy of methane in silicalite single crystals, e.g., 4.8 kJ/mol[17] and 4.0 kJ/mol.[18] This might be because of the contribution of molecules existing in noncrystalline spaces during the measured diffusion time. The portion of molecules in the noncrystalline spaces becomes larger as the temperature increases; θ changed from 0.23 (173 K) to 0.11 (243 K). This means that the contribution of the diffusivity in noncrystalline spaces to the apparent diffusivity becomes larger at higher temperatures. In the long-time diffusion measurement, the diffusivity is obtained as a consequence of the diffusion in both spaces; thus, the temperature dependence of diffusivity might be different from that in the crystal.

The diffusivity is related to the root-mean-square displacement (RMSD) via the Einstein relation, $D = \langle r^2(t)\rangle/(6t)$. The results are shown in Figure 6 at various temperatures. The diffusivities at all temperatures in this figure show rapid initial decay and then become constant with an increase in the RMSD. The RMSD at which the diffusivity starts to decrease is used to deduce the distance between transport barriers.[16,21] Mitra et al.[21] proposed the formulation to explain the correlation of long-time diffusivity with short-time diffusivity of fluid in porous media. According to their model, the diffusivity starts to drop much earlier than the barrier spacing. Although the formulation could not represent the observed rapid decay of diffusivity with an increase in the displacement, as shown in Figure 6, it implies

that the distance between transport barriers is larger than 6 μm. This value is larger than the smallest dimension of the crystal in the membrane. Consequently, there is a possibility that the intercrystalline region works as a transport barrier

By assuming that the long-time diffusivity is an apparent diffusivity in the membrane, the flux of methane could be estimated using permeation theory.[5,6,8] In the theory, the estimation of flux is derived from a combination of an adsorption isotherm and a corrected diffusivity based on a surface diffusion model. The flux is fundamentally expressed by Fick's law, and the Fickian diffusivity, D_F, in the relationship is correlated with a corrected diffusivity, D_0, as $D_F = D_0(\partial \ln q/\partial \ln p)$ through Darken's equation. Here, q is the amount of loading and p is the gas pressure. For methane in silicalite, D_0 is independent of loading and $D_0 \approx D_s$ can be derived because D_0 is equal to a self-diffusivity within the limit of dilute loading.[8] This approximation would be reasonable, especially in this study, because our permeation test has been carried out at relatively low loading conditions. The expression $\partial \ln q/\partial \ln p$ is equal to $(1 - \theta)^{-1}$ when a Langmuir equation for the description of the adsorption−pressure relationship of methane in silicalite is assumed. Finally, when the pressure on the permeate side is approximated to be zero and the Langmuir equation is used, the flux, J, through a zeolite membrane is expressed as follows:

$$J = \frac{\rho D_s q_m}{p_0 L} \ln(1 + K_A p_0) \quad (4)$$

where ρ is the density of the membrane, K_A and q_m are the Langmuir parameters, L is the membrane thickness (50 μm), and p_0 is the feed pressure (1.01×10^{-5} Pa). We used a silicalite density as ρ. The K_A and q_m used in this study are taken from our previous report.[22] The calculated flux at 300 K via eq 4 with apparent diffusivity ($D_s = 3.7 \times 10^{-9}$ m^2/s) is 8.9×10^{-7} mol m^{-2} s^{-1} Pa^{-1}. This value is a factor of 6 larger than the experimental value of this membrane, 1.4×10^{-7} mol m^{-2} s^{-1} Pa^{-1}. The apparent diffusivity of the membrane enumerated backward from eq 4 using the experimental flux is 0.58×10^{-9} m^2/s.

Let us consider the reason for the discrepancy between the diffusivity data produced by PFG-NMR and the permeation test. Although the discrepancy between theoretical and experimental values has often been explained as a result in an error in the estimation of membrane thickness, this is not true in this study because it is unrealistic to propose that the actual membrane thickness is six times thicker than that estimated from an SEM image. The inaccuracy in the Langmuir parameters used and the density of the membrane would be a partial reason for the overestimation of the flux. The surface of the membrane far from the support layer consists of dense crystals, while the crystals close to the support layer have a relatively sparse structure,[14] which leads to reduction in the membrane density compared with that of a single crystal. The relatively low crystallinity implied from the slightly small BET measurement data would change the Langmuir parameters. However, it is difficult to conclude that these errors can completely explain the observed significant discrepancy in diffusivity, which might provide evidence for the existence of another factor that reduces the flux.

Conclusion

^{1}H PFG spin−echo NMR was carried out to measure the diffusivity of methane in polycrystalline silicalite. Measured diffusivities decreased with an increase in the diffusion time and distance. This result suggests the presence of a transport barrier in the membrane. The distance between the transport barriers would be larger than 6 μm; this value is derived from the relationship of diffusivity with RMSD. The estimated distances are larger than the smallest dimension of the crystals appearing in the membrane surface.

The transport barrier at intercrystalline regions in A-type membranes has been proposed by Heink[4] for hydrocarbons. The small diffusivity in zeolite membranes as compared with that in intracrystalline regions seems to be a general feature in polycrystalline zeolite membranes. In our study, the apparent diffusivity of methane in the silicalite membrane was smaller by a factor of 3 than that in a single crystal. The previously measured long-time diffusivity of methane in silicalite crystallites, which experienced the transport barrier at the outer surface of the crystal, under the same measuring conditions showed almost the same value (2×10^{-9} to 3×10^{-9} m^2/s at 223 K)[3]. This implies a similarity in the origin of the decrease in diffusivity in these systems. Since the magnitude of the decrease in diffusivity in zeolite membranes may depend on the diffusing species, further study is needed to discuss the variation in diffusivity.

Although the estimated flux using measured long-time diffusivity with the permeation theory overestimated the experimental value, it is closer to the experimental value than the value estimated using the short-time diffusivity. The methane diffusivity in the membrane is estimated to be 0.58×10^{-9} m^2/s from the permeation test, which is still much smaller than the long-time diffusivity from NMR (3.7×10^{-9} m^2/s). It is noted that the estimation via eq 4 using the diffusivity in single crystals, as shown in Table 1, [6,23,25] gives significantly larger flux values, 2.6×10^{-6} to 3.8×10^{-6} mol m^{-2} s^{-1} Pa^{-1}, and the use of the apparent diffusivity closes the gap between the theoretical estimation via eq 4 and the experimental value. These results mean that the consideration of the difference between diffusivity in a single crystal and that in membranes is crucial in the theoretical estimation of zeolite membrane performance.

References and Notes

(1) Kärger, J.; Ruthven, D. M. *Diffusion in Zeolites and Other Microporous Solids*; Wiley: New York, 1992.
(2) Vasenkov, S.; Bohlmann, W.; Galvosas, P.; Geier, O.; Liu, H.; Karger, J. *J. Phys. Chem. B* **2001**, *105*, 5922−5927.
(3) Takaba, H.; Yamamoto, A.; Hayamizu, K.; Oumi, Y.; Sano, T.; Akiba, E.; Nakao, S. *Chem. Phys. Lett.* **2004**, *393*, 87−91.
(4) Heink, W.; Kärger, J.; Naylor, T.; Winkler, U. *Chem. Commun.* **1999**, *1*, 57−58.
(5) Nagumo, R.; Takaba, H.; Suzuki, S.; Nakao, S. *Microporous Mesoporous Mater.* **2001**, *48*, 247−254.
(6) Suzuki, S.; Takaba, H.; Yamaguchi, T.; Nakao, S. *J. Phys. Chem. B* **2000**, *104*, 1971−1976.
(7) Pohl, P. I.; Heffelfinger, G. S.; Smith, D. M. *Mol. Phys.* **1996**, *89*, 1725−1731.
(8) Bowen, T. C.; Falconer, J. L.; Noble, R. D.; Skoulidas, A. I.; Sholl, D. S. *Ind. Eng. Chem. Res.* **2002**, *41*, 1641−1650.
(9) Sano, T.; Yanagishita, H.; Kiyozumi, Y.; Mizukami, F.; Haraya, K. *J. Membr. Sci.* **1994**, *95*, 221−228.
(10) Lai, Z. P.; Bonilla, G.; Diaz, I.; Nery, J. G.; Sujaoti, K.; Amat, M. A.; Kokkoli, E.; Terasaki, O.; Thompson, R. W.; Tsapatsis, M.; Vlachos, D. G. *Science* **2003**, *300*, 456−460.
(11) Lovallo, M. C.; Tsapatsis, M. *AIChE J.* **1996**, *42*, 3020−3029.
(12) Stejskal, E. O.; Tanner, J. E. *J. Chem. Phys.* **1965**, *42*, 288.
(13) Oumi, Y.; Miyajima, A.; Miyamoto, J.; Sano, T. *Stud. Surf. Sci. Catal.* **2002**, *142*, 1595−1602.
(14) Nomura, M.; Yamaguchi, T.; Nakao, S. *J. Membr. Sci.* **1998**, *144*, 161−171.
(15) Kärger, J.; Walter, A. *Z. Phys. Chem. (Leipzig)* **1974**, *255*, 142−148.
(16) Geier, O.; Snurr, R. Q.; Stallmach, F.; Karger, J. *J. Chem. Phys.* **2004**, *120*, 367−373.

(17) Jobic, H.; Bee, M.; Kearley, G. J. *Zeolites* **1989**, *9*, 312−317.
(18) Caro, J.; Bulow, M.; Schirmer, W.; Kärger, J.; Heink, W.; Pfeifer, H.; Zdanov, S. P. *J. Chem. Soc., Faraday Trans.* **1985**, *81*, 2541−2550.
(19) June, R. L.; Bell, A. T.; Theodorou, D. N. *J. Phys. Chem.* **1990**, *94*, 8232−8240.
(20) Talu, O.; Sun, M. S.; Shah, D. B. *AIChE J.* **1998**, *44*, 681−694.
(21) Mitra, P. P.; Sen, P. N.; Schwartz, L. M. *Phys. Rev. B* **1993,** *47*, 8565−8574.
(22) Nagumo, R.; Takaba, H.; Nakao, S. *J. Phys. Chem. B* **2003**, *107*, 14 422−14 428.